Letter

Unexpected scaling of interstitial velocities with permeability due to polymer retention in porous media

Shima Parsa,[1,2,3,*] Ahmad Zareei,[1,*] Enric Santanach-Carreras,[4,5] Eliza J. Morris,[1,6] Ariel Amir,[1] Lizhi Xiao,[7,2,†] and David A. Weitz[1,8,2,‡]

[1]*John A. Paulson School of Engineering and Applied Sciences, Harvard University, Cambridge, Massachusetts 02138, USA*

[2]*Harvard SEAS-CUPB Joint Laboratory on Petroleum Science, Cambridge, Massachusetts 02138, USA*

[3]*School of Physics and Astronomy, Rochester Institute of Technology, Rochester, New York 14623, USA*

[4]*Total SA, Pôle d'Etudes et Recherche de Lacq, BP 47-64170 Lacq, France*

[5]*Laboratoire Physico-Chimie des Interfaces Complexes, Total SA-ESPCI-CNRS, Route Départementale 817, 64170 Lacq, France*

[6]*Department of Physics and Astronomy, California State University, Sacramento, California 95819, USA*

[7]*State Key Laboratory of Petroleum Resources and Prospecting, China University of Petroleum, Beijing 102249, China*

[8]*Department of Physics, Harvard University, Cambridge, Massachusetts 02138, USA*

(Received 8 February 2021; accepted 26 July 2021; published 25 August 2021)

Polymer retention from the flow of a polymer solution through porous media results in substantial decrease of the permeability; however, the underlying physics of this effect is unknown. While the polymer retention leads to a decrease in pore volume, here we show that this cannot cause the full reduction in permeability. Instead, to determine the origin of this anomalous decrease in permeability, we use confocal microscopy to measure the pore-level velocities in an index-matched model porous medium. We show that they exhibit an exponential distribution and, upon polymer retention, this distribution is broadened yet retains the same exponential form. Surprisingly, the velocity distributions are scaled by the inverse square root of the permeabilities. We combine experiment and simulation to show these changes result from diversion of flow in the random porous-medium network rather than reduction in pore volume upon polymer retention.

DOI: 10.1103/PhysRevFluids.6.L082302

The flow and transport of fluids and material in a porous medium is ubiquitous in many industrial and environmental applications such as oil recovery, water filtration, soil remediation, chromatography, and CO_2 sequestration [1,2], and understanding this behavior is essential to improve any of these applications. This becomes especially important, and particularly difficult, when the pore structure changes dynamically due to the flowing fluids, as occurs, for example, in the case of enhanced oil recovery with polymer flooding, biofilm growth in water filters, and adsorption of nanoparticles and mineral precipitation in rocks [3–16]. Because of the highly disordered pore structure in porous media [1,2,17], the flow is distributed between pores in complex ways [17–21], making a full understanding much more difficult to achieve. The average flow can be understood; it is well described by a mean-field approximation, Darcy's law, which is a linear relation between

*These authors contributed equally to this work.
†xiaolizhi@cup.edu.cn
‡weitz@seas.harvard.edu

pressure drop and average flux through the medium. However, there is considerable heterogeneity in the flow beyond the mean-field approximation, and this significantly impacts transport through the medium [22–26]. Such local heterogeneity in transport can be exacerbated when the network structure changes dynamically [4,7]. These changes in network structure often result from a change in porosity such as in immiscible displacement [27], or in bioclogging where pores are completely filled [7,8]; in both cases the permeability of the medium is clearly reduced. By contrast, in other cases such as the flow of polymer solutions, there are no clear changes in the structure of the medium or in the porosity; nevertheless dramatic changes of the permeability and the average flow are observed [3–5,28]. Even the flow of small amounts of polymer can have significant effects; while there is retention of polymer in the porous medium, the amount is insufficient to lead to the significant change in porosity that would be required to change the permeability within the mean-field approximation [3]. Thus the origin of these large effects of polymer on the flow in porous medium remains unclear. This lack of understanding limits our ability to optimize the dispersion of polymers used in soil treatment [29] or in polymer enhanced oil recovery [3].

In this Letter, we identify the origin of the large impact of flow of a polymer solution on the permeability of a porous medium. We use confocal microscopy to measure the pore-level velocities in an index-matched model porous medium made of a glass-bead pack. We show that the initial distribution of velocities is exponential in form. Polymer retention alters the local pore connectivity in the disordered structure resulting in large changes in fluid transport through the porous medium; these changes lead to the decrease in permeability, which results in an increase in the average flow velocity when the volumetric flow rate remains constant. Surprisingly, however, the experimentally measured shape of the distribution of pore-level velocities remains exponential although it is broadened substantially. Remarkably, the average velocity of the fluid flow scales with the inverse of the square root of the measured permeability upon polymer retention; moreover, the probability distributions of the velocities can also be scaled by this factor. Simulations of fluid flow through a network of tubes which models the experimental porous medium yield similar pore-level velocity distributions and the same scaling with permeability and confirm that these changes in permeability are a result of changes in network connectivity as the retained polymer begins to successively block the narrowest tubes.

We prepare a three-dimensional (3D) micromodel porous medium from a random loose packing of borosilicate glass beads with radii $R = 75\ \mu$m in a square quartz capillary with a cross-sectional area of $A = 3 \times 3$ mm^2 and a length of $L = 4$ cm. The beads are sintered to form a solid with a porosity of $\phi_0 = 48\%$. We prepare a polymer solution using Flopaam 3630 (SNF), a commercial-grade, partially hydrolyzed, linear polyacrylamide with a molecular weight of 20M Da, which is used extensively in oil recovery [3]. The polymer is dissolved at 5 g/l in deionized water along with salt, NaCl, at 7 g/l. To modify the viscosity, glycerol is added to yield a polymer solution of 1.6 g/l; the resultant solution is shear thinning with a zero-shear rate viscosity of 50 mPas. We use a syringe pump to flow the polymer solution into the medium at 50 μl/h which is sufficiently slow to avoid any shear induced thinning of the polymer solution even where the flow is highest [30,31]. To characterize the properties of the porous medium, we replace the polymer solution with a strictly Newtonian fluid, formulated to have the same index of refraction as the glass beads, which allows direct visualization of fluids within the medium with optical microscopy. The index-matched fluid is a mixture of 85% glycerol, 8% dimethyl sulfoxide, and 7% water by weight, and has a viscosity of $\mu = 160$ mPas [32]. A schematic of the experimental setup is shown in Fig. 1(a).

We quantify the impact of flow of polymer solution on bulk transport properties through the porous medium by measuring its permeability, k, as we vary the total volume of polymer that flows through the porous medium. We use the index-matched fluid to measure the permeability before and after flow of a fixed volume of polymer solution, measured in units of the pore volume of the porous medium. The permeability is determined by varying the flow rate, Q, and measuring pressure drop, ΔP, using a transducer (Omegadyne PX409), and using Darcy's law (see Supplemental Material [33] for data). The initial permeability of the medium is $k_i = 4.7 \times 10^{-11}$ m^2; it decreases significantly, as much as 60%, to $k_f = 1.4 \times 10^{-11}$ m^2 with increasing polymer flow as shown in

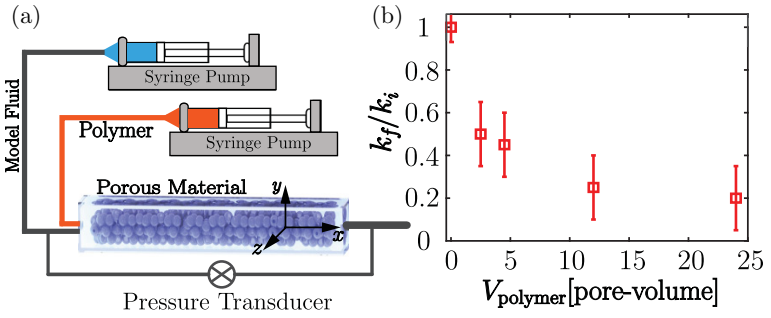

FIG. 1. Measurement of the bulk permeability of the porous medium. (a) Schematic of the experimental apparatus. Fluid flow is controlled by syringe pumps and resultant pressure across the medium is monitored by a transducer. (b) Relative changes in permeability k_f/k_i after flow of polymer solution, V_{polymer}. Error bars represent the standard deviation of several measurements.

Fig. 1(b). Interestingly, most of the decrease occurs with the initial polymer flow; the permeability is already reduced by 50% after five pore volumes. The reduction in permeability implies that polymer is retained in the medium, consistent with results of measurements with the same polymer in single capillary tubes [34].

We quantify the pore-level velocities within the medium prior to polymer flow using confocal microscopy and particle image velocimetry (PIV). The index-matched fluid is seeded with 1-μm-diameter fluorescent latex tracer particles at 0.01% by volume and flowed into the medium at $Q = 200$ μl/h. This flow rate is strictly within the laminar regime as reflected by the low Reynolds number, the ratio of inertial to viscous forces, which is of the order of 10^{-6}. Furthermore, diffusion of the tracer particles is negligible at this flow rate since their Péclet number, the relative strength of advection to diffusion, is of the order of 10^5. Particle-particle interactions are negligible at this low concentration and there is negligible retention of the particles in the porous medium. There is no measurable impact on the rheological properties of the index-matched fluid (see Supplemental Material [33] for measured viscosity). For high-resolution PIV, we acquire movies of 300 frames at 15 Hz at a fixed position a few glass bead diameters deep into the medium. Each image spans a lateral area of 911×911 μm^2 and has a depth of field of 11 μm. We determine the average pore-level velocity in the image plane using PIV at a resolution of 4×4 μm^2, and repeat this to determine the pore-level flow velocities over the whole sample at this fixed depth [35]. We display the spatial distribution of these velocities in a heat map where the beads are clearly seen by black circles; the magnitude of the velocity varies by more than a factor of 10 across the sample and there are noticeable spatial correlations as shown in Fig. 2(a).

To quantify the variability in the pore-level velocities within the medium, we determine their probability density function (PDF). The PDF is well described by an exponential distribution, which reflects the relatively small number of extremely large velocities, as shown in Fig. 3(a). This is similar to earlier measurements in 3D micromodels [7,35]. We also measure the average pore-level velocity $u_i = 14.8$ μm/s; this is close to the average interstitial velocity, $u_{\text{int}} = Q/(\phi_0 A)$, which is calculated to be $u_{\text{int}} = 12.9$ μm/s.

To quantify the impact of polymer retention on the local fluid velocities, we flow 12 pore volumes of the polymer solution through the porous medium. We then displace the polymer solution with the index-matched fluid and then add tracer particles to perform PIV measurements at the same sample depth. Variations in the magnitude of the pore-level velocities are exacerbated after the polymer flow, with pores having larger velocities being significantly more abundant as shown by the heat map in Fig. 2(b). The average velocity increases to $u_f = 25.2$ μm/s, consistent with the reduction in permeability due to polymer retention. Interestingly, while some pores experience much larger fluid flow velocities, others have similar or even reduced flow velocities, which is most clearly seen

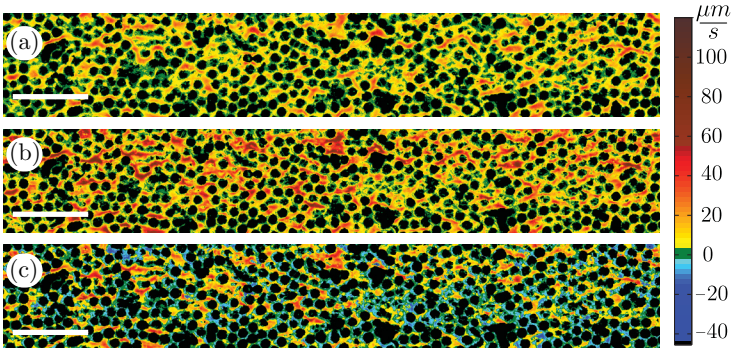

FIG. 2. Heat map of magnitude of the fluid velocity in a 2D plane within the 3D porous medium, for a flow rate of 200 μl/h (a) before and (b) after 12 pore volumes of polymer flow, showing increased local velocities. (c) Difference between the longitudinal components of velocity before and after polymer flow showing heterogeneous changes in local velocity due to polymer retention. Black circles represent glass beads. Scale bars are 1 mm.

by the difference in the longitudinal components of velocities, Δu_L, the direction of the bulk fluid flow. Many regions exhibit increased longitudinal velocities $\Delta u_L > 0$; surprisingly, however, some pores have decreased velocities where $\Delta u_L < 0$, as clearly seen in the heat map shown in Fig. 2(c). Interestingly, a few pores even have their flow direction reversed, as seen in a heat map of the angle between the direction of velocities before and after (see Supplemental Material [33] for the heat map). These data clearly show that the changes in local flow due to polymer retention are extremely heterogeneous with wide variations between different pores. We also observe strong correlations in Δu_L that can extend over several pores. However, these measurements are only in a two-dimensional slice of the micromodel and these correlations may differ in 3D. To quantify the impact of polymer retention on the distribution of local velocities, we compare the PDF of the magnitude of the fluid velocities before and after polymer flow. Surprisingly, the PDF of the magnitude of velocities after polymer flow remains exponential in form, although the tail of the distribution becomes broader as seen in Fig. 3(a). We also measure the PDF for another sample, made in an identical fashion but where we increase the total amount of polymer flowed through the sample by using 20 pore

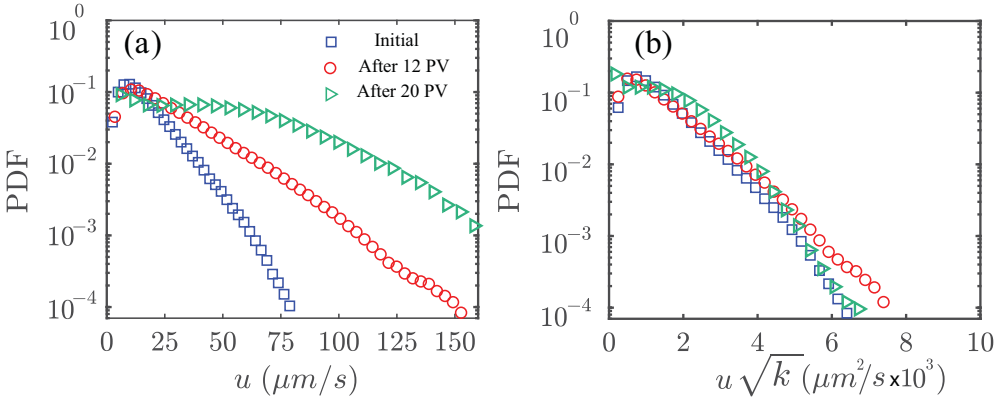

FIG. 3. Probability density function (PDF) of the magnitude of fluid flow velocities (a) before polymer (blue squares) and after flow of 12 pore volumes of polymer (PV) (red circles), and after 20 pore volumes (green triangles), and (b) scaling of behavior when normalized by $1/\sqrt{k}$.

volumes of the polymer solution. The PDF of velocities is again exponential, albeit with some deviation reflecting the additional uncertainty in the PIV measurement as shown in Fig. 3(a).

Further insights into the origin of the changes of pore-level velocities upon polymer retention can be obtained by considering the dependence of the average velocity on the permeability, which changes upon polymer retention. Since the permeability reflects the resistance to flow which is dominated by the throat size we use a dimensional argument: To a good approximation, the permeability of a bead pack is the square of the throat size formed between the beads, typically 1/10 of the diameter of beads; thus, for example, the permeability of the model porous medium before polymer flow is calculated to be 2.2×10^{-10} m^2 which is a reasonable approximation for the measured value of 4.7×10^{-11} m^2, given the qualitative nature of this approach. An even better approximation is obtained using the Kozeny-Carman relation to calculate the permeability for a packing of monodisperse spheres of known porosity; we obtain 5×10^{-11} m^2, in excellent agreement with the measured value. However, the origin of this dimensional dependence arises because the resistance of flow of a throat depends on its diameter to the fourth power, but the permeability also depends on the number of throats in the cross-sectional area, which in turn depends inversely on the square of the bead diameter, leading to the observed scaling of permeability with bead size. However, upon polymer retention it is only the throat diameter that can be changed, not the separation, hence, for fixed flow rate, the change in velocity should scale inversely as the square root of permeability. To be more precise, we model the permeability using N parallel tubes with length L and diameter d at separation l, and assume Poiseuille flow in each tube to determine the permeability. In this network the pressure drops, ΔP, for all the parallel tubes are the same, while the total flux is distributed between them. The flux in each tube is $Q_{\text{tube}} = (\pi d^4 \Delta P)/(128\mu L)$. Hence, the volumetric flow rate in the medium is $Q = (\pi A \Delta P d^4)/(128\mu l^2 L)$; here $A = Nl^2$ is the total cross-sectional area, assuming $d \ll l$. By comparison with Darcy's law, $Q = (kA\Delta P)/(\mu L)$, the permeability of this network of parallel tubes is $k = \pi d^4/128l^2$. The average interstitial velocity is the ratio of the volumetric flow rate to area, $U = 4Q/\pi d^2$. Thus, $Q \sim U\sqrt{k}$ and at constant volumetric flow rate,

$$U \propto \frac{1}{\sqrt{k}}. \tag{1}$$

To test this prediction, we scale the PDF of the velocities by the square roots of the inverse permeabilities. The scaled PDFs all collapse upon one another, with no fitting parameters, as shown in Fig. 3(b).

This scaling behavior has important consequences. It means that even though the interstitial velocity cannot be directly measured without determining pore-level velocities, it can, nevertheless, be calculated from the permeability, which can be measured with bulk methods.

Polymer retention clearly changes the permeability of the porous medium; however, the effect on the porosity is not clear. Because the permeability is decreased, the porosity must also be decreased; however, we cannot determine this decrease through the optical measurements. Instead, we can use the measured average interstitial velocity to determine the modified porosity ϕ_{eq}, using $U = Q/(\phi_{\text{eq}}A)$, which gives $\phi_{\text{eq}} = 28\%$. This value seems unreasonably low; if the porosity were to decrease so much, we would be able to measure it optically. Moreover, if we assume a random packing of spheres, their radius would have to increase by 10% to account for the change in porosity; this corresponds to a polymer coating nearly 8 μm thick which is unreasonably large given that the radius of gyration of the polymer is about 200 nm. Alternatively, we can use the measured change in permeability upon polymer retention and calculate the expected value of porosity for a packing of monodisperse spherical beads using the Kozeny-Carman equation; we find $\phi = 38\%$. This value is also unreasonably low as it would require a polymer thickness of 4 μm, which is again unreasonably large. Thus, the effects of polymer flow cannot be the result of only a reduction in porosity due to polymer retention; instead, it must reflect the consequences of the highly disordered fluid flow network and its wide distribution of pore and throat sizes.

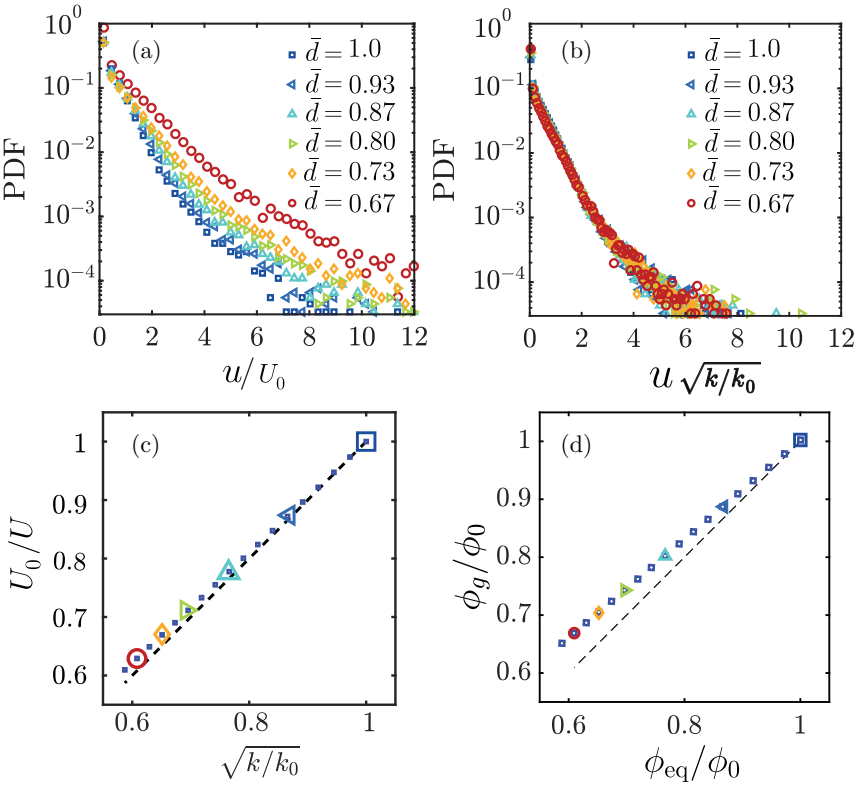

FIG. 4. (a) Probability density function (PDF) of the magnitude of flow velocities, normalized by the U_0, for different values of average tube diameter. (b) PDF normalized by the inverse square root of the permeability. (c) The relation between relative average velocity in the network U/U_0 and the inverse square root of permeability $\sqrt{k/k_0}$ calculated directly from simulation. (d) Comparison between geometric porosity and equivalent porosity, measured from average velocity, as the diameters of tubes are reduced.

While our experiments determine the change in pore-level velocity due to polymer retention, they are unable to directly measure any change in the porosity, and are thus unable to provide insight into the effects of disorder on the underlying origin of the changes. Instead, we use numerical simulation. We model the porous medium with 30 000 nodes randomly located in a plane and each connected by a tube to all its neighbors as delimited through a Delaunay triangulation. The tubes have a random diameter and we assume Poiseuille flow in each tube and solve for conservation of mass at each junction [19,36–40]. Modeling a bead pack with a network of tubes with a wide distribution of diameters is known to robustly capture the flow statistics [19]. Even though the beads are monodisperse, their porosity is 48%, well above that of a random close packing of monodisperse spheres. In this case the distribution of pores is very broad [41–43] as reflected by the exponential distribution of velocities. Consistent with this, when we numerically examine several distributions of diameters, we find that the PDF of flow velocities always exhibits an exponential form (see Supplemental Material [33] for PDF of velocity). We assume that the diameters of all tubes decrease an equal amount upon polymer retention and study the effects as the average tube diameter normalized by the initial value, $\bar{d}$, is reduced. When any tube diameter is reduced to zero, we assume it is completely blocked; an increasing number of tubes are blocked with increasing polymer retention. In all cases the distribution of pore-level velocities remains exponential in shape, although with a noticeable tail at high velocities, as shown in Fig. 4(a). The heat map of the calculated velocities in the network exhibits behavior similar to that of the experiment: there is

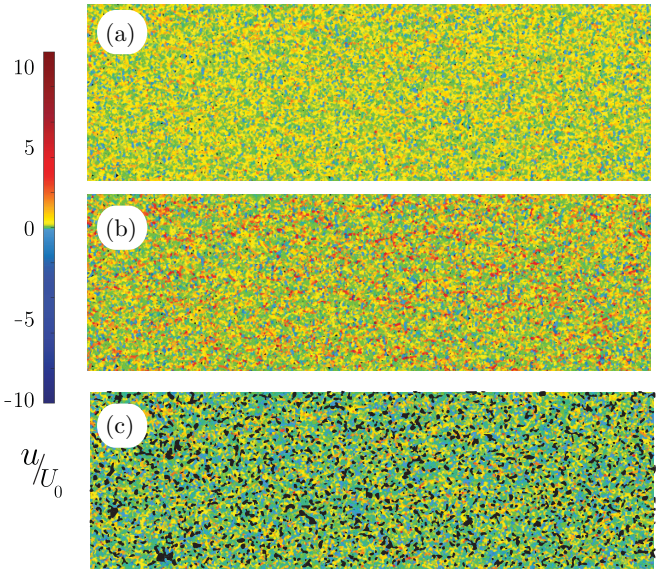

FIG. 5. Heat map of magnitude of velocities (a) before and (b) after reduction of tube diameters, $\bar{d} = 0.67$. (c) Difference between the longitudinal component of velocities before and after reduction in tube diameter highlighting heterogeneity in changes in local flow. Blocked pores shown in black.

a wide range of velocities and these increase significantly upon polymer retention, as can be seen by comparing the behavior for $\bar{d} = 1$ with that for $\bar{d} = 0.67$ in Figs. 5(a) and 5(b). Just as for the experiment, the difference in longitudinal velocity displays many tubes where u_L is decreased significantly as seen in the lower panel of Fig. 5(c). However, in the simulation we can identify the blocked tubes which are shown in black. The permeability for each network is determined from the ratio of the flow rate and applied pressure using Darcy's law. The velocity PDFs scale onto a single master curve when normalized by the ratio of the square root of the permeabilities, exactly as observed experimentally, as shown in Fig. 4(b). This scaling dependence is further highlighted by the linear relation between the normalized average velocity and the square root of ratio of the permeabilities shown in Fig. 4(c). We can determine the effective porosity due to polymer retention from the calculated average interstitial velocity; however, from the simulations, we can determine the precise geometric porosity due to the reduction in the tube diameter. These values deviate from one another with increasing polymer retention as shown by the difference between the measured ϕ_g, shown by the data, and the value of ϕ_{eq}, shown by the solid line, in Fig. 4(d). This deviation is direct evidence confirming that the large change in interstitial velocity upon polymer retention is due to modification of the complex fluid flow network rather than the changes in the porosity. This suggests that the most important effect in polymer retention is in blocking some of the pores, or otherwise modifying the network flow.

The experimental measurements and numerical simulations presented here quantify the impact of polymer retention on the pore-level velocity distribution and porous medium permeability. The unexpectedly large decrease in permeability due to polymer retention is a direct result of blockage and diversion of flow throughout the network of the porous medium rather than an overall reduction in pore sizes due to polymer retention. The consequences of these effects are highlighted by the scaling of the velocity distributions with the inverse square root of the permeability. This scaling also provides a valuable means of determining the interstitial velocity even when it cannot be measured directly as is typically the case in most applications of porous media geometries. These results provide important new insights into the underlying origin of the modification of flow in porous

media due to polymer retention and can serve as an essential contribution to any attempt to improve the effects of polymer flow in porous media.

It is a pleasure to acknowledge K. Alim for stimulating discussion. This work was supported by the Harvard University Materials Research Science and Engineering Center under NSF awards DMR-2011754 and DMR-1708729, Total E&P Recherche Developpement awards FR00006025, FR00006847, and FR00007513, the Kavli Institute for Bionano Science and Technology, and China University of Petroleum, Beijing China 111 project B13010.

[1] J. Bear, *Dynamics of Fluids in Porous Media* (Courier Corporation, North Chelmsford, MA, 2013).
[2] M. Sahim, *Flow and Transport in Porous Media and Fractured Rock: From Classical Methods to Modern Approaches* (Wiley, New York, 2011).
[3] L. W Lake, R. Johns, B. Rossen, and G. A. Pope, *Fundamentals of Enhanced Oil Recovery* (Society of Petroleum Engineers, Richardson, TX, 2014).
[4] S. Parsa, E. Santanach-Carreras, L. Xiao, and D. A. Weitz, Origin of anomalous polymer-induced fluid displacement in porous media, Phys. Rev. Fluids **5**, 022001(R) (2020).
[5] P. Barreau, D. Lasseux, H. Bertin, P. Glenat, and A. Zaitoun, An experimental and numerical study of polymer action on relative permeability and capillary pressure, Pet. Geosci. **5**, 201 (1999).
[6] D. Levitt, S. Jouenne, I. Bondino, J. Gingras, and M. Bourrel, The interpretation of polymer coreflood results for heavy oil, SPE 150566 (2011), doi: 10.2118/150566-MS.
[7] M. Carrel, V. L. Morales, M. A. Beltran, N. Derlon, R. Kaufmann, E. Morgenroth, and M. Holzner, Biofilms in 3D porous media: Delineating the influence of the pore network geometry, flow and mass transfer on biofilm development, Water Res. **134**, 280 (2018).
[8] J. D. Seymour, J. P. Gage, S. L. Codd, and R. Gerlach, Anomalous Fuid Transport in Porous Media Induced by Biofilm Growth, Phys. Rev. Lett. **93**, 198103 (2004).
[9] K. Drescher, Y. Shen, B. L. Bassler and H. A. Stone, Biofilm streamers cause catastrophic disruption of flow with consequences for environmental and medical systems, Proc. Natl. Acad. Sci. USA **110**, 4345 (2013).
[10] A. Tran-Viet, A. F. Routh, and A. W. Woods, Control of the permeability of a porous media using a thermally sensitive polymer, AIChE J. **60**, 1193 (2014).
[11] D. Levitt, S. Jouenne, I. Bondino, E. Santanach-Carreras, and M. Bourrel, Polymer flooding of heavy oil under adverse mobility conditions, SPE 165267 (2013), doi: 10.2118/165267-MS.
[12] C. Huh and G. A. Pope, Residual oil saturation from polymer floods: Laboratory measurements and theoretical interpretation, SPE-113417 (2008), doi: 10.2118/113417-MS.
[13] J. S. Vrouwenvelder, C. Hinrichs, W. G. J. Van der Meer, M. C. M. Van Loosdrecht, and J. C. Kruithof, Pressure drop increase by biofilm accumulation in spiral wound RO and NF membrane systems: Role of substrate concentration, flow velocity, substrate load and flow direction, Biofouling **25**, 543 (2009).
[14] M. Rolle, C. Eberhardt, G. Chiogna, O. A. Cirpka, and P. Grathwohl, Enhancement of dilution and transverse reactive mixing in porous media: Experiments and model-based interpretation, J. Contam. Hydrol. **110**, 130 (2009).
[15] M. Norouzi Rad, N. Shokri, and M. Sahimi, Pore-scale dynamics of salt precipitation in drying porous media, Phys. Rev. E **88**, 032404 (2013).
[16] G. Gerber, M. Bensouda, D. A. Weitz, and P. Coussot, Self-Limited Accumulation of Ccolloids in Porous Media, Phys. Rev. Lett. **123**, 158005 (2019).
[17] M. Siena, A. Guadagnini, M. Riva, B. Bijeljic, J. P. Pereira Nunes, and M. J. Blunt, Statistical scaling of pore-scale Lagrangian velocities in natural porous media, Phys. Rev. E **90**, 023013 (2014).
[18] R. S Maier, D. M. Kroll, Y. E. Kutsovsky, H. T. Davis, and R. S. Bernard, Simulation of flow through bead packs using the lattice Boltzmann method, Phys. Fluids **10**, 60 (1998).

[19] K. Alim, S. Parsa, D. A. Weitz, and M. P. Brenner, Local Pore Size Correlations Determine Flow Distributions in Porous Media, Phys. Rev. Lett. **119**, 144501 (2017).
[20] A. D. Araújo, W. B. Bastos, J. S. Andrade, Jr., and H. J. Herrmann, Distribution of local fluxes in diluted porous media, Phys. Rev. E **74**, 010401(R) (2006).
[21] J. K. Arthur, D. W. Ruth, and M. F. Tachie, PIV measurements of flow through a model porous medium with varying boundary conditions, J. Fluid Mech. **629**, 343 (2009).
[22] D. L. Koch and J. F. Brady, Anomalous diffusion in heterogeneous porous media, Phys. Fluids **31**, 965 (1988).
[23] B. Berkowitz, A. Cortis, M. Dentz, and H. Scher, Modeling non-Fickian transport in geological formations as a continuous time random walk, Rev. Geophys. **44**, RG2003 (2006).
[24] B. Bijeljic, P. Mostaghimi, and M. J. Blunt, Signature of Non-Fickian Solute Transport in Complex Heterogeneous Porous Media, Phys. Rev. Lett. **107**, 204502 (2011).
[25] Y. Edery, A. Guadagnini, H. Scher, and B. Berkowitz, Origins of anomalous transport in heterogeneous media: Structural and dynamic controls, Water Resour. Res. **50**, 1490 (2014).
[26] T. Le Borgne, M. Dentz, and E. Villermaux, Stretching, Coalescence, and Mixing in Porous Media, Phys. Rev. Lett. **110**, 204501 (2013).
[27] S. Berg, H. Ott, S. A. Klapp, A. Schwing, R. Neiteler, N. Brussee, A. Makurat, L. Leu, F. Enzmann, J. O. Schwarz, M. Kersten, S. Irvine, M. Stampanoni, Real-time 3D imaging of Haines jumps in porous media flow, Proc. Natl. Acad. Sci. USA **110**, 3755 (2013).
[28] P. Zitha, G. Chauveteau, and L. Léger, Unsteady-state flow of flexible polymers in porous media, J. Colloid Interface Sci. **234**, 269 (2001).
[29] R. E. Sojka, D. L. Bjorneberg, J. A. Entry, R. D. Lentz, and W. J. Orts, Polyacrylamide in agriculture and environmental land management, Adv. Agron. **92**, 75 (2007).
[30] A. Clarke, A. M. Howe, J. Mitchell, J. Staniland, and L. A. Hawkes, How viscoelastic polymer flooding enhances displacement efficiency, SPE-174654 (2015), doi: 10.2118/174654-MS.
[31] C. A. Browne, A. Shih, and S. S. Datta, Pore-scale flow characterization of polymer solutions in microfluidic porous media, Small **16**, 1903944 (2019).
[32] I. Bischofberger, R. Ramachandran, and S. R. Nagel, Fingering versus stability in the limit of zero interfacial tension, Nat. Commun. **5**, 5265 (2014).
[33] See Supplemental Material at http://link.aps.org/supplemental/10.1103/PhysRevFluids.6.L082302 for experimental procedures and additional data.
[34] C. A. Grattoni, P. F. Luckham, X. D. Jing, L. Norman, and R. W. Zimmerman, Polymers as relative permeability modifiers: Adsorption and the dynamic formation of thick polyacrylamide layers, J. Pet. Sci. Eng. **45**, 233 (2004).
[35] S. S. Datta, H. Chiang, T. S. Ramakrishnan, and D. A. Weitz, Spatial Fluctuations of Fluid Velocities in Flow through a Three-Dimensional Porous Medium, Phys. Rev. Lett. **111**, 064501 (2013).
[36] I. Fatt, The network model of porous media, Trans. AIME **207**, 144 (1956).
[37] D. Fraggedakis, E. Chaparian, and O. Tammisola, The first open channel for yield-stress fluids in porous media, J. Fluid Mech. **911**, A58 (2021).
[38] M. J. Blunt, B. Bijeljic, H. Dong, O. Gharbi, S. Iglauer, P. Mostaghimi, A. Paluszny, and C. Pentland, Pore-scale imaging and modelling, Adv. Water Resour. **51**, 197 (2013).
[39] N. Stoop, N. Waisbord, V. Kantsler, V. Heinonen, J. S. Guasto, and J. Dunkel, Disorder-induced topological transition in porous media flow networks, J. Non-Newtonian Fluid Mech. **268**, 66 (2019).
[40] S. L. Bryant, P. R King, and D. W. Mellor, Network model evaluation of permeability and spatial correlation in a real random sphere packing, Transp. Porous Media **11**, 53 (1993).
[41] M. Yanuka, F. Dullien, and D. E. Elrick, Percolation processes and porous media: I. Geometrical and topological model of porous media using a three-dimensional joint pore size distribution, J. Colloid Interface Sci. **112**, 24 (1986).
[42] M. M. Roozbahani, L. Graham-Brady, and J. D. Frost, Mechanical trapping of fine particles in a medium of mono-sized randomly packed spheres, Int. J. Numer. Anal. Methods Geomech. **38**, 1776 (2014).
[43] M. M. Roozbahani, R. Borela, and J. D. Frost, Pore size distribution in granular material microstructure, Materials **10**, 1237 (2017).